

Optimization of the snowflake diverted equilibria in the TCV tokamak

S.Yu. Medvedev¹, A.A. Ivanov¹, A.A. Martynov¹, Yu.Yu. Poshekhanov¹,
 Y.R. Martin², J-M. Moret², F. Piras², A. Pochelon², H.Reimerdes², O. Sauter², L. Villard²
 and the TCV team

¹*Keldysh Institute, Russian Academy of Sciences, Moscow, Russia*

²*Ecole Polytechnique Fédérale de Lausanne (EPFL), Centre de Recherches en Physique des Plasmas, Association Euratom-Confédération Suisse, Lausanne, Switzerland*

In support of the TCV experimental campaign aiming at studying H-mode plasmas with snowflake (SF) divertor [1, 2], free boundary equilibrium and stability studies were performed with the SPIDER [3] and KINX [4] codes. Due to the high flexibility of plasma shaping capabilities of TCV, SF divertor conditions can be reached for various plasma geometries. However, at high plasma current some configurations require poloidal field (PF) coil currents close to the machine limit. This is particularly important when the equilibrium sensitivity to the edge pedestal profiles, which is higher than for standard X-point configurations, is taken into account. That is why the configuration optimization should also include the profile sensitivity study when planning the shot scenario.

1 Inverse equilibrium problem with prescribed nulls of the poloidal field

The equilibrium code SPIDER (reconstruction mode) [3] has been modified to compute free boundary equilibria with prescribed positions of either two X-points or a single second order null of the poloidal magnetic field for SF configurations. The separatrix strike point positions can also be controlled, in particular so that they match with the regions fully covered by graphite tiles and avoid the ports positions at the outer wall: this is particularly important for snowflake and negative triangularity plasmas in TCV. The values of PF coil currents are minimized and the TCV hardware constraints are checked.

The following functional is used for the least square fit of the prescribed fitting points (r_l, z_l) , i.e. target plasma shape:

$$W = \sum_{l=1}^L \omega_l \left[\psi_p(r_l, z_l) + \sum_{k=1}^K J_k G(r_l, z_l; r_k, z_k) - \psi_{boun} \right]^2 + \sigma \sum_{k=1}^K d_k (J_k - J_k^{ref})^2. \quad (1)$$

The PF coil current values J_k and the boundary poloidal flux value ψ_{boun} are varied to minimize the functional. The parameter $\sigma > 0$ provides the regularization. The coefficients ω_l and d_k are used to control the fitting accuracy for individual points and deviations of individual PF coil currents from the prescribed reference values J_k^{ref} . The $\psi_p(r_l, z_l)$ are the plasma current generated poloidal flux values in the fitting points, and $G(r_l, z_l; r_k, z_k)$ are the values of Green function of the Grad-Shafranov operator Δ^* .

The limiter points, satisfying the requirement that the plasma boundary passes strictly through them (including the X-points and the second order null) are treated using Lagrange multipliers. It was found that prescribing two X-points very close (typically $|\Delta\vec{r}|/|\vec{r}| < 10^{-5}$) to each other gives almost same result as the direct prescription of the second order null position within the accuracy of the equilibrium solution on the numerical grid. The coding is easier for more versa-

tile inverse equilibrium version with prescribed X-point positions, because only first derivatives of the Green function enter the conditions $\partial\psi/\partial r = 0$, $\partial\psi/\partial z = 0$ at the X-points, while two additional conditions at the second order null $\partial^2\psi/\partial z^2 = 0$, $\partial^2\psi/\partial r\partial z = 0$ (then $\partial^2\psi/\partial r^2 = 0$ due to $\Delta^*\psi = 0$ in vacuum) involve the second derivatives .

2 Free boundary SF equilibria under variations of plasma profiles

The following procedure was proposed for the optimization of TCV shots with a SF divertor. The EXPEQ file with the results of the TCV equilibrium reconstruction with the LIUQE code is a starting point of the procedure. The values of currents in the PF coils are not taken from LIUQE but reconstructed by running the SPIDER code in the inverse equilibrium mode with the plasma profiles and the target plasma shape taken from the EXPEQ. For the sensitivity study the profiles are replaced with the conventional TCV pedestal profiles [5]. Then the TCV hardware requirements are checked. In order to satisfy the requirements, the PF currents reconstruction is repeated under a special choice of the weights in the functional (1).

In particular, for the equilibrium for the TCV shot #43418 at time 0.8s (plasma current $I_p = 263kA$) was reproduced with the SPIDER as shown in Fig.1a. The distance between the X-points measured in units of the plasma minor radius is 0.25 for the initial equilibrium. The next step is to replace the X-point with the larger Z coordinate (R, Z) = (0.79, -0.123) by the second order null. The SF equilibrium with the original LIUQE profiles (Fig.1b) leads to admissible PF coil currents with the weights $\omega_l = 1$ for all the fitting points and $d_k = 1$ for all the PF coil currents and $\sigma = 20$ in the regularization functional (1). It can be compared to the equilibrium with the TCV pedestal profiles. The plasma profile change leads to larger PF currents and violation of the MGAMS protection condition for the TCV hardware (Fig.1c). The weights d_k were tuned to relax dipoles in E and F coils (the weights for the E4, F3, F4 and F5 coils multiplied by 5) together with higher overall weight $\sigma = 60$ for better minimization of the PF coil currents, sacrificing the plasma shape control.

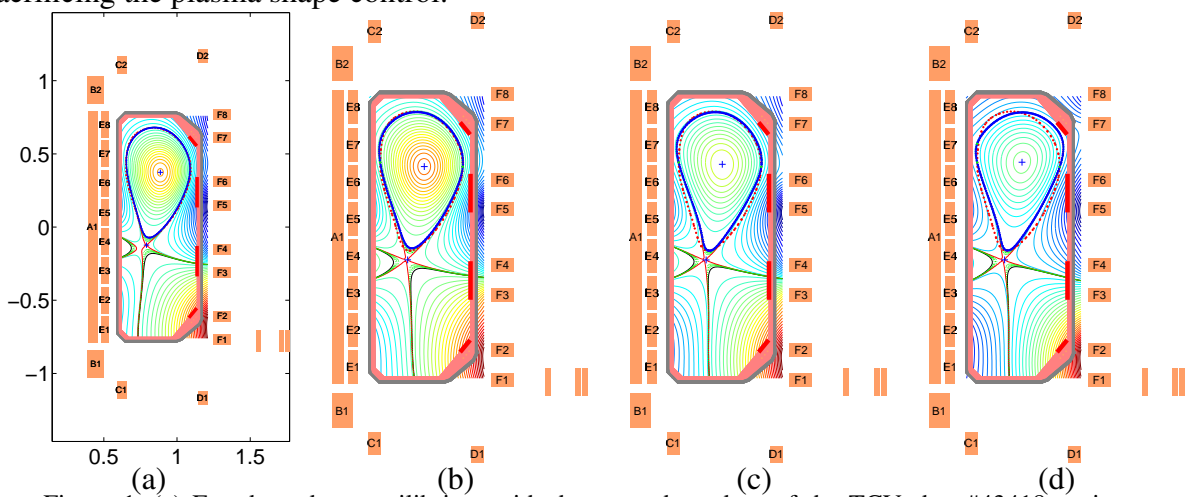


Figure 1. (a) Free boundary equilibrium with the target boundary of the TCV shot #43418 at time 0.8s, $I_p = 263kA$: SPIDER reconstruction, original X-point positions (0.79,-0.123), (0.74,-0.15). (b) SF equilibrium with second order null at (0.79,-0.123) and with the LIUQE profiles. (c) SF equilibrium with pedestal profiles (MGAMS protection violated). (d) SF equilibrium with pedestal profiles, tuned weights in the functional. The positions of full toroidal coverage zones with graphite tiles are shown by thick red lines.

It results in lower triangularity of the plasma top (Fig.1d) and MGAMS protection condition satisfied. In addition to the target plasma shape from the LIUQE reconstruction, three limiter points (marked by green dots in Fig.1d) were prescribed in order to keep the plasma minor radius approximately constant.

In the next series of the equilibrium calculations, while keeping the target shape fixed, the positions of either SF or two X-points were varied. In Fig.2 the maximal currents in the PF coils (by absolute value, per turn) are shown versus the second order null radial position ($Z = -0.123$) for the SF equilibria or the second X-point radial position ($Z = -0.15$, the first X-point was always at (0.79,-0.123)). The tuned weights in the functional are used. As expected the values of the PF coil currents are minimal when the X-points are close either to E or F coils. Note that the position of the SF point at the low field side (LFS), that corresponds to the negative triangularity of the null point, is also within the TCV hardware capabilities.

The $n = 0$ growth rates were computed with the KINX code for the equilibrium series corresponding to the Fig.2a. A significant vertical stability enhancement with the pedestal profiles (almost a factor of 2) can be observed both for the SF and two X-point cases. The value of the internal inductance is higher for the LIUQE current density profile as compared to the pedestal one: $l_i = 1.0$ vs $l_i = 0.75$. However, as shown in [2], the stabilization is mostly due to the modification of the plasma boundary near the shallow minimum of the poloidal field for high current density in the pedestal.

The equilibria with the second order null and the second X-point at LFS ($R_{X2} = 1.09$) are shown in Fig.3a and Fig.3b respectively.

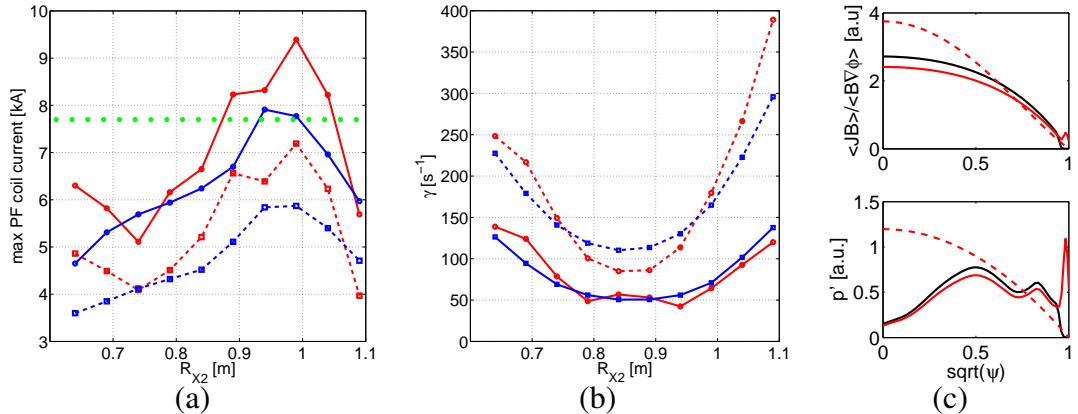


Figure 2. (a) Maximal PF coil currents for the SF (red) and two X-point (blue) equilibria versus the second order null radial position ($Z_{SF} = -0.123$) and the second X-point radial position ($Z_{X2} = -0.15$, the first X-point coordinates are $R_{X1} = 0.79$, $Z_{X1} = -0.123$) radial coordinate respectively; solid lines - pedestal profiles, dashed lines - LIUQE profiles. The TCV limit 7.7kA is shown by green dots. (b) The $n = 0$ growth rates with the resistive TCV wall of the equilibria with the corresponding SF and the second X-point positions. (c) The parallel current density and pressure gradient profiles with pedestal (solid red lines, internal inductance $l_i = 0.75$), from LIUQE (dashed red, $l_i = 1.0$) and with zero pedestal (solid black, $l_i = 0.85$).

Finally, the sensitivity of the SF equilibria to the profiles is demonstrated by the splitting of the second order null when the pedestal height drops, e.g. during the ELM cycle (see the profiles

in Fig.2c) under fixed values of the PF coil and plasma currents. The resulting spread of the X-points is 0.25 in units of the minor radius (Fig.3c and Fig.3d).

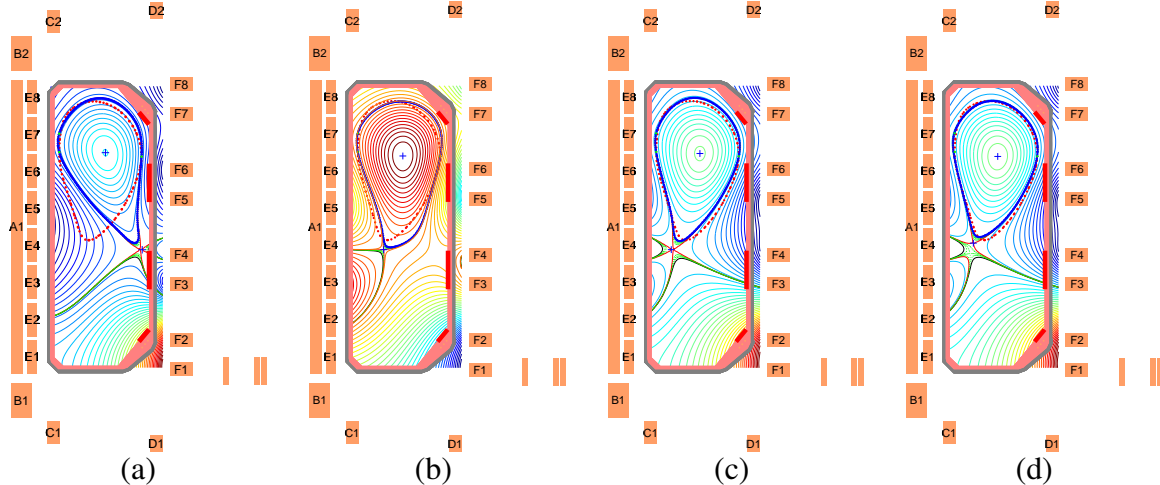


Figure 3. (a) The equilibrium with the SF point position $(R_{SF}, Z_{SF}) = (1.09, -0.123)$, pedestal profiles. (b) The equilibrium with the second X-point position $((R_{X2}, Z_{X2}) = (1.09, -0.15)$, pedestal profiles. (c) Nearly optimal equilibrium with the SF point position $(R_{SF}, Z_{SF}) = (0.74, -0.123)$, pedestal profiles. (d) The equilibrium with PF coil currents for the equilibrium (c) but with the zero pedestal profiles.

The elongation of the plasma decreases from 1.7 to 1.6, but the $n = 0$ growth rate is higher: $\gamma = 78\text{s}^{-1}$ and $\gamma = 100\text{s}^{-1}$ respectively. The internal inductance is higher for the current density profile without pedestal ($l_i = 0.85$), which is destabilizing. However the equilibrium with the pedestal profiles ($l_i = 0.75$) but in the same boundary from Fig.1d gives $\gamma = 90\text{s}^{-1}$, confirming the stabilizing effect of narrowing of the boundary near the null points due to high current density in the pedestal (even combined with increased elongation).

3 Discussion

The shots with SF divertor in TCV demonstrated advantageous features with respect to the ELM frequency and the distribution of the heat flux over divertor legs [1]. The experimental location of the poloidal field nulls is not far from the optimal one in terms of the PF coil currents. With the radial position of the second order null at $R = 0.74m$ and lower upper triangularity it is possible to reach the exact SF configuration with the pedestal profiles in H-mode. However active feedback control would be needed to maintain the second order null under profile variations.

Enhanced vertical stability of the SF configurations with the pedestal profiles, including the configurations with two nearby X-points, due to the plasma boundary deformation in the divertor region is an additional advantage as compared to the single X-point case. The stabilizing effect of the perturbed surface currents for strongly up-down nonsymmetric plasma cross-sections can be verified in the SF experiments.

- [1] F.Piras *et al.* Phys. Rev. Lett. **105**, 155003 (2010)
- [2] S.Yu.Medvedev *et al.* 37th EPS Conf. on Plasma Phys. ECA Vol.34A, P4.144 (2010)
- [3] A.A. Ivanov *et al.* KIAM Preprint #39, Moscow, 2009
http://www.keldysh.ru/papers/2009/prep39/prep2009_39.pdf
- [4] L. Degtyarev *et al.* Comput. Phys. Commun. **103**(1997)10
- [5] R. Behn *et al.* Plasma Phys. Control. Fusion **49** (2007) 1289

The CRPP authors are supported in part by the Swiss National Science Foundation.